Audio Engineering Society

Convention Paper 10308

Presented at the AES 160th Convention
2026 May 28–30, Copenhagen, Denmark

This paper was peer-reviewed as a complete manuscript for presentation at this convention. This paper is available in the AES E-Library (http://www.aes.org/e-lib), all rights reserved. Reproduction of this paper, or any portion thereof, is not permitted without direct permission from the Journal of the Audio Engineering Society.

Measurement Uncertainty of MEMS Microphone Sensitivity in A Free-Field Condition

Teguh Aditanoyo[1], Salvador Barrera-Figueroa[2], Jonas Brunskog[1], and Frieder Lucklum[1]

[1]*Centre for Acoustic-Mechanical Microsystems (CAMM), DTU Electrical and Photonics Engineering, Technical University of Denmark (DTU), 2800 Kgs. Lyngby, Denmark*
[2]*Danish Fundamental Metrology A/S, 2970 Hørsholm, Denmark*

Correspondence should be addressed to Teguh Aditanoyo (tegad@dtu.dk)

ABSTRACT

This work presents a measurement uncertainty evaluation of the free-field sensitivity of a MEMS microphone using a substitution comparison method. The measurement setup is based on principles used in secondary microphone calibration, with sensitivity determined relative to a calibrated reference microphone. The uncertainty analysis follows the Guide to the Expression of Uncertainty in Measurement (GUM), where Type A and Type B uncertainty evaluations are propagated through a defined measurement model to obtain the final measurement result. The MEMS microphone sensitivity is estimated together with an expanded uncertainty, where the uncertainties associated with the reference microphone are identified as the dominant contributors. Broadband results show that the measured sensitivity is close to the typical manufacturer sensitivity over a wide frequency range and follows a similar frequency trend. The proposed approach enables reproducible estimation of the free-field sensitivity of MEMS microphones and provides a clear framework for uncertainty evaluation.

1 Introduction

The purpose of this work is to demonstrate the evaluation of measurement uncertainty in determining the free-field sensitivity of a MEMS microphone using a comparison method. The measurement setup is inspired by the procedure for secondary microphone calibration described in IEC 61094-8 and its practical implementation in [1]. The setup is described in detail to support reproducibility. A primary free-field calibration procedure for MEMS microphones has previously been investigated in [2].

Over recent decades, microphones have continuously decreased in size, and MEMS microphones have become sufficiently reliable for compact devices such as earphones, headsets, and hearing aids. Characterization of microphone sensitivity in free-field conditions (e.g., in an anechoic chamber) is commonly performed by manufacturers to evaluate performance and guide product design. In addition, the present setup enables high-precision handling of MEMS microphones and makes possible future measurements inside compact acoustic cavity for which conventional condenser microphones are unsuitable.

According to the Guide to the Expression of Uncertainty in Measurement (GUM) [3], a measurement result is an estimate of the value of a measurand and must be accompanied by a statement of uncertainty. The main objective of this paper is therefore to determine the free field sensitivity of a MEMS microphone

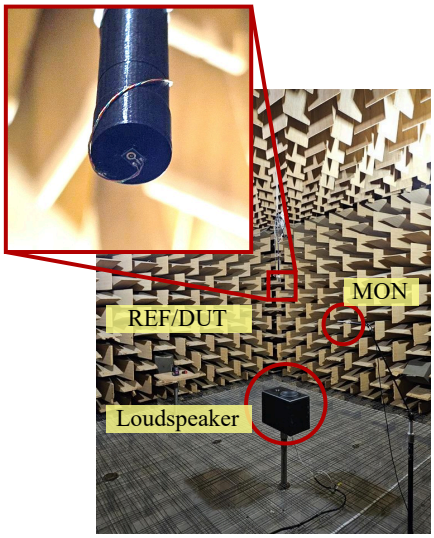


Fig. 1: Measurement setup in an anechoic chamber. A zoomed picture of the MEMS mic, which is attached to a 1/2" black rod

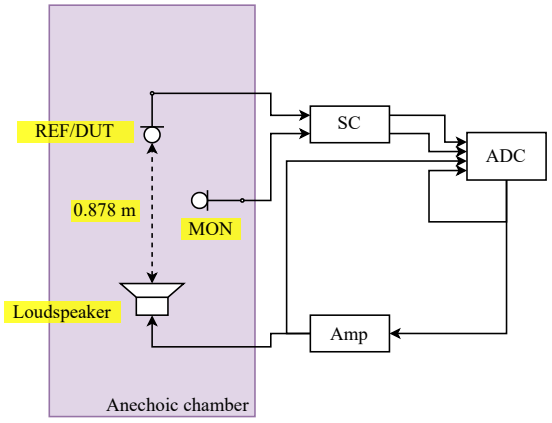


Fig. 2: Connection diagram of the setup

together with its associated measurement uncertainty. This work addresses uncertainty in the measurement procedure and not product reliability nor production tolerance.

It is important to clarify terminology. The term microphone sensitivity used in this work does not refer to the metrological definition of sensitivity given in the International Vocabulary of Metrology (VIM) [4]. Instead, it refers to the electroacoustic transfer function of the microphone that converts sound pressure fluctuations into electrical voltage.

2 Method and setup of the comparison method

2.1 Measurement model

The device under test (DUT) is a MEMS microphone (P11AC03, Sonion, Denmark). Its free-field sensitivity is determined relative to a calibrated reference microphone (REF) (Type 4191-L-001, Hottinger Brüel Kjær, Denmark) using a substitution comparison method. A loudspeaker generates a sound pressure signal that is first measured by the REF. The REF is then replaced by the DUT at the same position and exposed to the same acoustic field. A schematic of the setup is shown in Figure 1.

In the ideal case, the loaded sensitivity of the DUT, S_{DUT}, is obtained from the known sensitivity of the reference microphone, S_{REF}, and the ratio of their output voltages

$$S_{\mathrm{DUT}} = S_{\mathrm{REF}} R_M, \qquad R_M = \frac{v_{\mathrm{DUT}}}{v_{\mathrm{REF}}}. \tag{1}$$

where v_{DUT} and v_{REF} is the output voltage of the DUT and REF microphones, respectively.

Microphone sensitivity is commonly expressed in decibels. The sensitivity level of the DUT, M_{DUT}, can be written as

$$M_{\mathrm{DUT}} = M_{\mathrm{REF}} + \Delta S, \qquad \Delta S = 20\log_{10}\left(\frac{|v_{\mathrm{DUT}}|}{|v_{\mathrm{REF}}|}\right). \tag{2}$$

where M_{REF} is the known free-field sensitivity level of the reference microphone in dB re 1 V/Pa.

For conventional condenser microphones, open-circuit sensitivity is usually determined. However, most MEMS microphones include an integrated preamplifier that cannot be separated from the sensing element. Therefore, the present work determines the *loaded sensitivity*.

To ensure that the measurement result is independent of the excitation signal and of the specific loudspeaker used, both microphone responses are normalized by the electrical signal driving the loudspeaker (see Fig. 2). The sensitivity is therefore determined from a ratio

of transfer functions rather than from absolute sound pressure. This formulation allows the procedure to be reproduced using arbitrary excitation signals and different loudspeakers, provided that the acoustic field remains stable during each substitution measurement. The sensitivity level is then obtained from the ratio of transfer functions

$$M_{\mathrm{DUT}} = M_{\mathrm{REF}} + 20\log_{10}\left(\frac{|H_{\mathrm{DUT,amp}}|}{|H_{\mathrm{REF,amp}}|}\right), \quad (3)$$

where $H_{\mathrm{DUT,amp}}$ and $H_{\mathrm{REF,amp}}$ denote the transfer functions between the loudspeaker drive signal and the measured microphone responses.

The transfer functions are estimated as

$$H_{\mathrm{DUT,amp}} = \frac{S_{\mathrm{DUT,amp}}}{S_{\mathrm{amp,amp}}}, \qquad H_{\mathrm{REF,amp}} = \frac{S_{\mathrm{REF,amp}}}{S_{\mathrm{amp,amp}}}. \quad (4)$$

where $S_{\mathrm{DUT,amp}}$ and $S_{\mathrm{REF,amp}}$ are the cross-spectra between the amplifier output and the DUT and REF microphone signals, respectively, and $S_{\mathrm{amp,amp}}$ is the autospectrum of the amplifier output signal.

Microphone protection grid factor, distance mismatch and environmental conditions are included in the measurement model as

$$M_{\mathrm{DUT}} = M_{\mathrm{REF}} + M_{\mathrm{grid}} + 20\log_{10}\left(\frac{|H_{\mathrm{DUT,amp}}|}{|H_{\mathrm{REF,amp}}|}\right) + 20\log_{10}\left(\frac{d_{\mathrm{REF}}}{d_{\mathrm{DUT}}}\right) + \delta_p\,(p-p_0) + \delta_t\,(t-t_0)\,. \quad (5)$$

where M_{grid} is the correction factor of the reference microphone's protection grid typical response [5], d_{REF} and d_{DUT} are the distances from the loudspeaker acoustic centre to the REF and DUT microphones, p and t are the measured static pressure and temperature, p_0 and t_0 is the reference static pressure and temperature, and δ_p and δ_t are corresponding static pressure and temperature coefficients of the reference microphone. This equation constitutes the measurement model linking the measurand M_{DUT} to all input quantities and forms the basis for uncertainty propagation.

The orientation of the microphones relative to the sound source may introduce additional error due to angular dependence of the free-field response. This effect is not included in the present model and is therefore treated as a potential source of additional uncertainty.

A monitor microphone (MON) is included to assess the stability of the acoustic field during substitution measurements. Its signal is *not* used in the present model, which therefore relies on the assumption of a stable acoustic field. The use of MON-based normalization and its implications for uncertainty are discussed in Section 4.

2.2 Measurement complex

Measurements were conducted in an anechoic chamber in order to approximate free-field conditions. The chamber minimizes reflections from surrounding surfaces and suppresses standing waves. The free-field cutoff frequency of an anechoic chamber is approximately 100 Hz, which therefore defines the lower frequency limit of the present study.

The DUT integrates the sensing element and an internal preamplifier within a surface-mount package of dimensions $3.35 \times 2.50 \times 1.29$ mm. According to the manufacturer specification, the typical sensitivity at 1 kHz is -35.5 dB re 1 V/Pa under a supply voltage of 0.9 V and a load impedance of 1 MΩ in parallel with less than 200 pF. Because the internal preamplifier cannot be separated from the sensing element, the microphone operates as an active sensor and the present work therefore determines the loaded sensitivity. The output impedance is approximately 4.5 kΩ. The input impedance of the signal conditioner is significantly larger than this value. Consequently, electrical loading effects on the measured sensitivity are negligible.

The MEMS microphone was mounted in a custom 3D-printed holder at the rod centre (Fig. 1). The holder matches the external geometry of the reference microphone. In substitution measurements, geometric differences can change the local acoustic pressure at the diaphragm due to reflection and scattering. Matching the dimensions reduces this systematic effect and improves comparability between REF and DUT. The MEMS microphone was powered by a size 312 hearing-aid battery.

The reference microphone sensitivity M_{REF}, given in the calibration sheet, is specified for free-field conditions *without* the protection grid. In this study, the grid was kept, as this reflects typical handling in practice. Its effect is included as a correction factor M_{grid} in the measurement model. This also allows the grid influence to be quantified, showing its magnitude and supporting decisions on grid removal for lower uncertainty.

The microphone–loudspeaker distance was 0.878 m, satisfying the far-field condition over the frequency range considered. The loudspeaker axis was aligned to the microphone at approximately 0° incidence using a laser alignment tool.

The excitation was a 10 s linear sine sweep from 15 Hz to 30 kHz. The signal was amplified by a class-D amplifier (D3020, NAD Electronics, Canada) and reproduced by a two-way loudspeaker (BM6, Dynaudio Acoustic, Denmark). Microphone signals were conditioned (Nexus 2690-A-0S4, Hottinger Brüel Kjær, Denmark) and then acquired (USB-4431, National Instruments, USA) at a sampling rate of 51.2 kHz.

Transfer functions were estimated using the Welch method. A Hann window with 66.7% overlap was applied, providing stable spectral estimates for broadband excitation signals such as sine sweeps.

To minimize positioning error, the manual substitution between REF and DUT microphones was performed carefully while maintaining the mounting position. Alignment was verified after each replacement and the distance was re-checked. The measurement sequence consisted of 20 REF measurements followed by 50 DUT measurements.

Environmental conditions were monitored throughout the experiment. Temperature and static pressure were recorded using a weather station (WXT536, Vaisala, Finland). The full measurement sequence was completed within approximately one hour in order to limit drift of environmental conditions and instrumentation.

All recorded data were inspected prior to uncertainty evaluation. Two conditions were treated as invalid measurement outcomes. The first was the occurrence of *measurement accidents*, such as impulsive disturbances caused by loud banging noise originating from nearby construction activity. The second was the presence of *large and irrelevant systematic effects*, for example those associated with abnormal operating conditions or extended measurement duration. When either condition was observed, the entire measurement sequence was discarded and repeated. Only measurement sets free from these effects were retained for uncertainty evaluation. The remaining data were assumed to be affected only by small systematic effects inherent to the setup and by random effects, which are subsequently treated within the uncertainty analysis.

3 Measurement result and uncertainty evaluation

3.1 Evaluation at 1 kHz

The free-field sensitivity of the MEMS microphone, M_{DUT}, is the measurand. Its true value is not known and cannot be determined exactly. The measurement result is therefore an estimate of the measurand obtained from the measurement model defined in Eq. (5), together with an associated uncertainty.

The measurement result is determined from multiple input estimates. Each input estimate corresponds to an underlying input quantity defined in the measurement model. However, only estimates of these quantities are observable and therefore enter the uncertainty analysis. Following the Guide to the Expression of Uncertainty in Measurement (GUM), uncertainties are classified as Type A, evaluated by statistical analysis of repeated observations, and Type B, evaluated by other means [3].

For each input estimate x_j, a standard uncertainty $u(x_j)$ is assigned. In the absence of correlation information, the input estimates are assumed to be uncorrelated for the purpose of uncertainty propagation. The combined standard uncertainty of the measurement result, $u_c(M_{\mathrm{DUT}})$, is obtained by propagation of uncertainties according to

$$u_c^2(M_{\mathrm{DUT}}) = \sum_{i=1}^{N} \left(\frac{\partial f}{\partial x_j} \right)^2 u^2(x_j). \tag{6}$$

where f is the measurement model and $c_i \equiv \partial f / \partial x_j$ is the corresponding sensitivity coefficients.

Measured input estimates may be associated with multiple uncertainty components. For example, repeated observations contribute to Type A uncertainty, while instrument specifications and calibration data contribute to Type B uncertainty. In the present work, these components are retained separately and propagated individually through the measurement model to improve transparency of the uncertainty budget. This is mathematically equivalent to combining the uncertainty components at the input-estimate level, as in the GUM example. The components are kept separate only to make their contributions easier to interpret and to help identification of dominant sources.

Table 1: Uncertainty budget for the free-field sensitivity of the MEMS microphone at 1 kHz

Input quantity X_j	Estimate x_j		Std. uncertainty $u(x_j)$			Sensitivity c_j	U. contribution $\lvert c_j \rvert u(x_j)$/dB	DoF ν_j
H_{DUT}	0.212	V/V	$u_{\mathrm{rep}}(H_{\mathrm{DUT}})$	1.89e-05	V/V	$\frac{20}{\ln 10}\,\frac{1}{\lvert H_{\mathrm{DUT,amp}} \rvert}$	0.000766	49
			$u_{\mathrm{ins}}(H_{\mathrm{DUT}})$	3.18e-05	V/V		0.00129	30
			$u_{\mathrm{res}}(H_{\mathrm{DUT}})$	4.86e-08	V/V		1.97e-06	100
H_{REF}	0.18	V/V	$u_{\mathrm{rep}}(H_{\mathrm{REF}})$	1.61e-05	V/V	$-\frac{20}{\ln 10}\,\frac{1}{\lvert H_{\mathrm{REF,amp}} \rvert}$,	0.000767	19
			$u_{\mathrm{ins}}(H_{\mathrm{REF}})$	3.18e-05	V/V		0.00151	30
			$u_{\mathrm{res}}(H_{\mathrm{REF}})$	7.68e-08	V/V		3.66e-06	100
M_{REF}	-36.5	dB	$u(M_{\mathrm{REF}})$	0.0537	dB	1	0.0537	5
M_{grid}	0.00847	dB	$u(M_{\mathrm{grid}})$	0.0997	dB	1	0.0997	30
d_{DUT}	0.878	m	$u_{\mathrm{rep}}(d_{\mathrm{DUT}})$	0.000192	m	$-\frac{20}{\ln 10}\,\frac{1}{d_{\mathrm{DUT}}}$	0.0019	2
			$u_{\mathrm{res}}(d_{\mathrm{DUT}})$	0.000167	m		0.00164	100
d_{REF}	0.878	m	$u_{\mathrm{rep}}(d_{\mathrm{REF}})$	0.000192	m	$\frac{20}{\ln 10}\,\frac{1}{d_{\mathrm{REF}}}$	0.0019	2
			$u_{\mathrm{res}}(d_{\mathrm{REF}})$	0.000167	m		0.00164	100
p	99.3	kPa	$u_{\mathrm{rep}}(p)$	0.00572	kPa	δ_p	4e-05	7
			$u_{\mathrm{ins}}(p)$	0.0144	kPa		0.000101	30
			$u_{\mathrm{res}}(p)$	0.00102	kPa		7.14e-06	100
t	292	K	$u_{\mathrm{rep}}(t)$	0.043	K	δ_t	8.59e-05	7
			$u_{\mathrm{ins}}(t)$	0.0866	K		0.000173	30
			$u_{\mathrm{res}}(t)$	0.0102	K		2.04e-05	100
p_0	99.3	kPa	$u(p_0)$	0.516	kPa	$-\delta_p$	3.62e-3	5
t_0	296	K	$u(t_0)$	0.447	K	$-\delta_t$	0.000894	5
δ_p	-0.007	dB/kPa	$u(\delta_p)$	0.00115	dB/kPa	$(p-p_0)$	5.27e-05	30
δ_t	-0.002	dB/K	$u(\delta_t)$	0.00115	dB/K	$(t-t_0)$	0.0053	30

Note: All values expressed in dB are referenced to 1 V/Pa.

The uncertainty budget at 1 kHz is summarized in Table 1.

The evaluation of the standard uncertainty associated with each input estimate at 1 kHz is described below.

Type A uncertainty evaluation

Several input estimates are obtained from repeated observations, namely H_{DUT}, H_{REF}, d_{DUT}, d_{REF}, p, and t. The standard uncertainty associated with repetition is denoted as $u_{\mathrm{rep}}(x_j)$. This notation is used to distinguish the repeatability contribution from other uncertainty components in the uncertainty budget table.

Following the GUM, the repeatability standard uncertainty is defined as

$$u_{\mathrm{rep}}(x_j) = s(\bar{X}_j),$$

where $s(\bar{X}_j)$ is the experimental standard deviation of the mean $\bar{X}_j$, obtained from n independent repeated measurements. As expected, increasing the number of repeated measurements reduces $u_{\mathrm{rep}}(x_j)$. The associated degrees of freedom are taken as $\nu_j = n-1$.

Type B uncertainty evaluation

Type B uncertainty components are evaluated from calibration data, instrument specifications, and numerical information provided in datasheets.

The calibration-related uncertainty of the reference microphone sensitivity M_{REF} is taken directly from the calibration certificate, together with its reported coverage factor. The reference static pressure p_0 and reference temperature t_0 are also taken from the calibration certificate, where their variances are provided. The effective

Table 2: Measurement result with its expanded uncertainty at 1 kHz

Measurand	Y	M_{DUT}	
Estimate	y	-34.964	dB re 1V/Pa
Combined variance	$u_c^2(M_{\mathrm{DUT}}) = \Sigma c_j^2 u^2(x_j)$	0.0130	(dB re 1 V/Pa)^2
Combined standard deviation	$u_c(M_{\mathrm{DUT}})$	0.114	dB re 1 V/Pa
Effective degrees of freedom	$\nu_{\mathrm{eff}}(M_{\mathrm{DUT}})$	33.5	
Level of confidence	p	95	%
t-factor	$t_p(\nu_{\mathrm{eff}})$	2.033	
Coverage factor	$k_p = t_p(\nu_{\mathrm{eff}})$	2.033	
Expanded uncertainty	$U_p = k_p u_c(M_{\mathrm{DUT}})$	0.231	dB re 1 V/Pa

degrees of freedom associated with these calibration-related uncertainties are assigned as $\nu_j = 5$, reflecting the high reliability of the calibration data.

For the grid correction factor M_{grid}, the uncertainty is assigned based on the reported typical frequency response [5]. The uncertainty is estimated by comparing the line thickness of the plotted response with the spacing of the plot axes. It is assumed that the line thickness represents the tolerance band. The resulting bounds are interpreted as limits of a rectangular distribution. An effective degrees of freedom $\nu_j = 30$ is assumed for this term.

For input estimates obtained using measuring instruments, two additional Type B uncertainty components are considered: instrument systematic uncertainty $u_{\mathrm{ins}}(x_j)$ and resolution uncertainty $u_{\mathrm{res}}(x_j)$.

The instrument systematic uncertainty $u_{\mathrm{ins}}(x_j)$ represents instrument-related effects that are not reduced by repeated measurements. For H_{DUT} and H_{REF}, the input noise of the data acquisition system specified in the datasheet is used and modeled with a rectangular distribution. For the environmental quantities p and t, the quoted $\pm$ accuracy values from the weather station datasheet are treated as instrument uncertainty and also modeled with a rectangular distribution. The associated degrees of freedom for instrument systematic uncertainty are assigned as $\nu_j = 30$.

The resolution uncertainty $u_{\mathrm{res}}(x_j)$ accounts for rounding effects. The data acquisition system provides a 24-bit resolution over a ± 10 V input range, corresponding to a voltage resolution of 1.19 nV, which affects the estimation of H_{DUT} and H_{REF}. The distances d_{DUT} and d_{REF} are measured using a ruler with a resolution of 1 mm. According to the weather station datasheet, the resolution is 0.01 kPa for static pressure and 0.1 K for temperature. All resolution-related uncertainties are modeled using rectangular distributions. Since rounding errors behave as random effects, the corresponding standard uncertainties are divided by $\sqrt{n}$, where n is the number of independent repeated observations.

Finally, numerical uncertainty associated with values taken from datasheets, specifically the static pressure coefficient δ_p and temperature coefficient δ_t, is considered. A conservative bound of twice the last reported digit is used, and a rectangular distribution is assumed. For both resolution-related and numerical uncertainty components, the effective degrees of freedom are assigned as $\nu_j = 100$.

Combined standard uncertainty

By plugging in the input estimates to the measurement model, the measurement result is calculated. The effective degrees of freedom is obtained from the Welch-Satterthwaite formula. Based on the uncertainty budget, its expanded uncertainty is defined as shown in Table 2.

Accordingly, the free-field sensitivity of the MEMS microphone at 1 kHz is reported as

$$M_{\mathrm{DUT}}(1\ \mathrm{kHz}) = (-34.96 \pm 0.23)\ \mathrm{dB\ re\ 1\ V/Pa},$$

where the uncertainty denotes the expanded uncertainty with a coverage factor of 95%.

Figure 3 shows the uncertainty contributions to the combined standard uncertainty at 1 kHz. The two largest

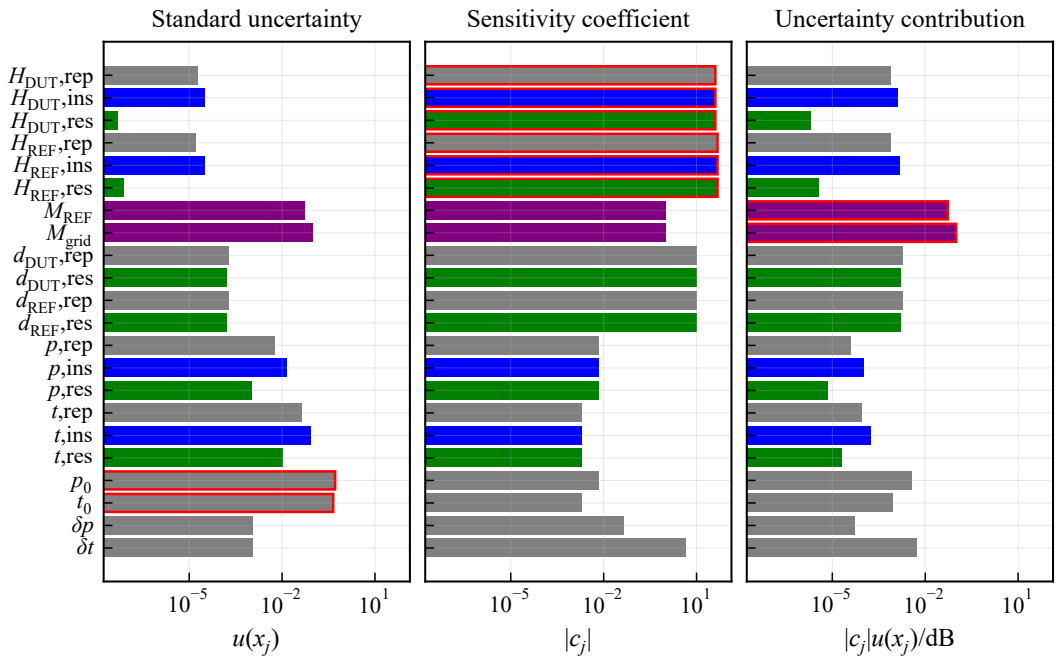


Fig. 3: Visualization of uncertainty budget for the free-field sensitivity of the MEMS microphone at 1 kHz: standard uncertainty from the input estimates, sensitivity coefficient, and the uncertainty contribution. Red outline signifies the biggest value of each category.

standard uncertainty components originate from the reference static pressure p_0 and the reference temperature t_0. The largest sensitivity coefficients are associated with the transfer functions $H_{\mathrm{DUT,amp}}$ and $H_{\mathrm{REF,amp}}$.

It is important to distinguish between standard uncertainty, sensitivity coefficient, and uncertainty contribution. Neither a large standard uncertainty nor a large sensitivity coefficient alone implies a dominant influence on the measurement result. The contribution to the combined uncertainty is determined by the product of both quantities. In the present case, the dominant contribution arises from the protection grid correction factor and calibration uncertainty of the reference microphone.

Identification of the dominant uncertainty contributions provides a basis for targeted improvement of the measurement setup. In this work, the expanded uncertainty is already sufficiently low for the intended application, and no further optimization is required within the current measurement model.

3.2 Broadband evaluation

The broadband sensitivity coefficients associated with the measurement model are shown in Fig. 4. The sensitivity coefficients vary with frequency and may take positive or negative values, depending on the sign of the partial derivative of the measurement model with respect to each input estimate.

Across most of the frequency range, the largest sensitivity coefficients are associated with the transfer functions $H_{\mathrm{DUT,amp}}$ and $H_{\mathrm{REF,amp}}$. These two sensitivity coefficients show a mirrored behaviour up to approximately 5 kHz. This observation is important, as it indicates that the dominant terms in the measurement model may affect the result in opposite directions.

In the present work, correlations between input estimates are not included in the uncertainty propagation. Nevertheless, the observed mirrored behaviour of the dominant sensitivity coefficients suggests that potential correlations between the transfer function estimates would partially cancel. Therefore, the assumption of

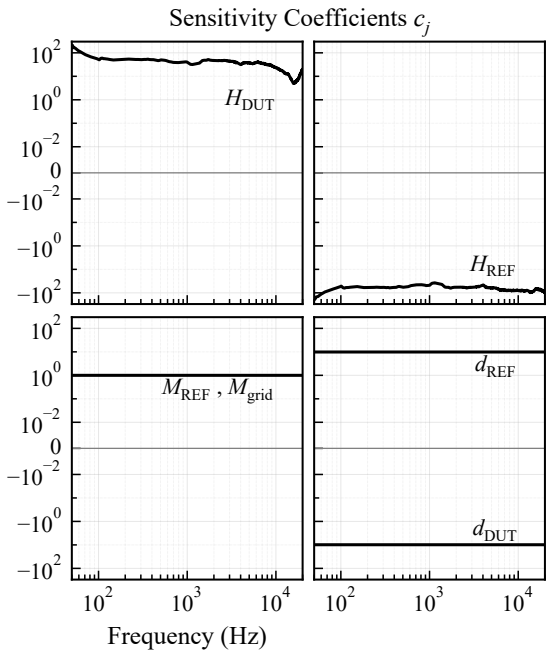


Fig. 4: Broadband sensitivity coefficients used in the uncertainty analysis. The coefficients for M_{REF} and M_{grid} are constant ($c_j = 1$, see Table 1). The coefficients related to source-to-microphone distances are assumed frequency independent. Environmental variables (p, t, p_0, t_0) and correction coefficients (δ_p, δ_t) are not shown and treated as frequency independent.

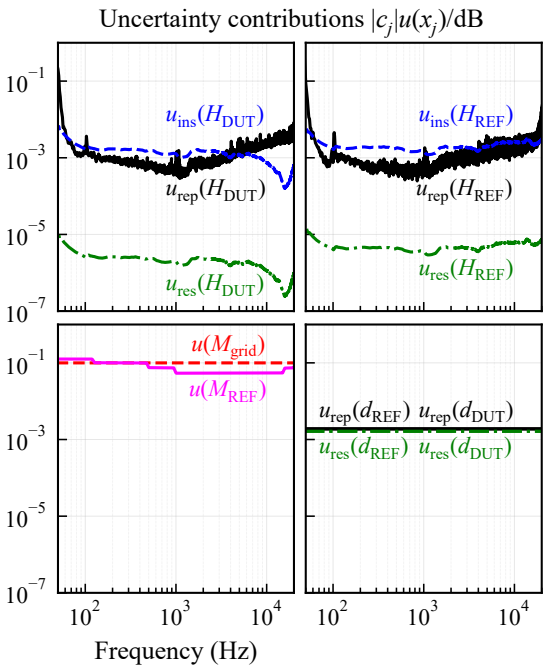


Fig. 5: Broadband uncertainty contributions. Black lines represent uncertainty due to repeated measurements, blue lines represent instrument-related uncertainty, and green lines represent resolution-related uncertainty. The dominant contributor is associated with M_{grid} grid correction factor and M_{REF} calibration uncertainty.

uncorrelated input estimates is considered reasonable for the frequency range where this behaviour is observed.

The sensitivity coefficients of M_{REF} and M_{grid} are frequency independent by definition of the measurement model. However, in the broadband evaluation, further simplifications are applied. The coefficients related to the source-to-microphone distances d_{DUT} and d_{REF} depend on the distance values and on the acoustic centre, which may vary with frequency. The coefficients of δ_p and δ_t are also frequency dependent. In this work, these quantities are treated as constant over frequency. Environmental quantities p, t, p_0, and t_0 are linked to coefficients defined by the reference microphone characteristics and are likewise assumed constant.

The frequency-dependent components of the combined standard uncertainty are shown in Fig. 5. Although the term *contribution* is not explicitly defined in the GUM, it is commonly used in metrology to describe the relative influence of individual uncertainty components on the combined uncertainty.

Over most of the frequency range, the dominant contribution originates from grid correction factor and the calibration uncertainty of the reference microphone. This behaviour is consistent with the results obtained at 1 kHz and confirms that the reference microphone characteristic limits the uncertainty of the present setup.

Below approximately 70 Hz, the uncertainty associated with the microphone transfer function estimates increases significantly. This frequency range lies below the free-field cutoff frequency of the anechoic chamber, where the assumptions of free-field propagation are no longer valid. As a result, the increased uncertainty in this region is attributed primarily to limitations of

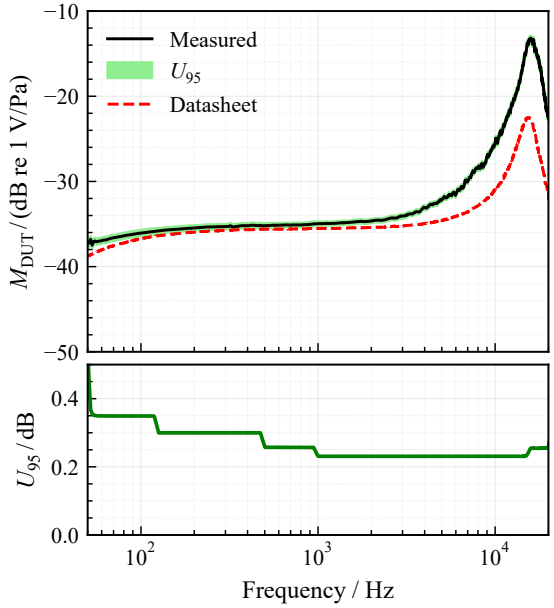


Fig. 6: Measured free field sensitivity of the MEMS microphone with its expanded uncertainty (coverage factor = 95%, k=2.03). Nominal value is taken from the manufacturer data sheet [6].

the measurement environment rather than to the microphones themselves.

The broadband free-field sensitivity of the MEMS microphone, together with its expanded uncertainty, is shown in Fig. 6. Between 100 Hz and 2 kHz, the measured sensitivity is close to the typical sensitivity specified by the manufacturer and follows a similar frequency trend. However, a systematic deviation is observed across the entire frequency range. The deviation is small at frequencies of a few hundred Hz but increases with frequency, becoming noticeable above approximately 2 kHz. At 10 kHz, the deviation reaches approximately 3 dB which exceeds the manufacturer tolerance of ± 1 dB, with even larger differences at higher frequencies. Several factors may contribute to this deviation.

First, the custom 3D-printed holder used for the DUT may interact with the acoustic field, particularly at shorter wavelengths where geometric and material effects become more apparent. Although the external dimensions of the holder were designed to match those of the reference microphone, the material properties and surface characteristics differ. For REF, the incident sound wave primarily interacts with the protection grid and diaphragm, which occupy most of the circular frontal area. In contrast, for the DUT assembly, a larger portion of the frontal surface is rigid, with only a small acoustic inlet of the MEMS microphone exposed to the incident wave. This difference may significantly alter the effective sound pressure at the sensing element.

Second, the manufacturer does not specify the measurement conditions used to determine the nominal free-field sensitivity. Differences in measurement setup or mounting conditions may therefore contribute to the observed deviation.

Finally, only a single MEMS microphone was measured in this work. It is possible that the tested device deviates from the typical sensitivity value. To further assess this effect, measurements on multiple microphones of the same type would be required. Based on the manufacturer specification, the expected unit-to-unit variation is within ± 1 dB.

Despite the observed deviation in sensitivity magnitude, the expanded uncertainty of the measurement result for this single microphone remains below 0.25 dB re 1 V/Pa over most of the frequency range between 1 kHz and 15 kHz. As mentioned previously, the broadband uncertainty is driven by the combination of the grid correction factor and calibration uncertainty of the reference microphone. The results therefore demonstrate high measurement precision, while the absolute accuracy is limited by systematic effects not fully accounted for in the present setup.

4 Discussion

The expanded uncertainty obtained in this work is sufficiently low for the intended application, demonstrating that the proposed measurement setup achieves high measurement precision and that the specific MEMS microphone tested operates reliably under the applied conditions. However, this result *cannot* be generalized to all MEMS microphones, as such a conclusion would require measurements on a larger sample of devices. In addition, further improvement would mainly require removing the protection grid and using a reference microphone with lower calibration uncertainty.

The measurement model is the central element of the uncertainty analysis, as it defines how all relevant input quantities are linked to the measurement result.

At the same time, the measurement model represents a limitation of the setup. If an input quantity is not explicitly included, its random effects are distributed among other input estimates through the measurement process, while any associated systematic effects remain unaccounted for. This highlights the importance of a comprehensive measurement model when interpreting both the measurement result and its uncertainty.

Several limitations of the measurement setup are identified. First, the measured free-field sensitivity of the MEMS microphone is inherently associated with the cylindrical rod and holder used in the present setup. Additional uncertainty contributions may arise from the mounting method, small geometric differences between the DUT holder and the reference microphone, and material-dependent acoustic effects. These effects were not quantified and may influence the high-frequency response.

Second, reproducibility was not explicitly evaluated. Factors such as changes in operator, repeated assembly and disassembly of the setup, and remounting of the MEMS microphone may introduce additional uncertainty. Previous studies on MEMS sensors have shown that mounting and reproducibility effects can be significant contributors to measurement uncertainty [7]. Quantifying these effects would improve the completeness of the uncertainty analysis.

Third, normalization using a monitor microphone was not investigated. While such normalization may reduce sensitivity to variations in the acoustic field, it may also introduce stronger correlations between input estimates. These correlations would require explicit treatment in the uncertainty propagation and may complicate the uncertainty analysis.

Finally, uncertainty contributions associated with spectral estimation were not analysed separately. Effects related to discrete Fourier transform processing, including windowing and spectral leakage, introduce both bias and variance [8]. These effects correspond to Type B and Type A uncertainty components, respectively, and are implicitly included in the present analysis. A dedicated investigation could further separate and quantify these contributions.

The uncertainty analysis presented in this work assumes uncorrelated input estimates. In practice, correlations may arise from shared instrumentation, time drift, or temperature sensitivity. For example, the reference and DUT signals are processed through the same signal conditioning and data acquisition hardware. Although this introduces potential correlation, the present work adopts an uncorrelated model for simplicity.

5 Conclusion

A measurement setup for determining the free-field sensitivity of a MEMS microphone using a substitution comparison method has been developed and implemented. The setup is based on principles used in secondary microphone calibration and is designed to enable high reproducibility of the measurement procedure.

The free-field sensitivity of the MEMS microphone was estimated together with an uncertainty evaluation following the GUM framework. The dominant contribution to the combined uncertainty originates from the grid correction factor and calibration uncertainty of the reference microphone.

The results show that the proposed setup provides a reliable estimate of MEMS microphone sensitivity in free-field conditions. The presented uncertainty analysis enables identification of dominant contributors and provides a basis for future refinement of the measurement method.

Acknowledgement The author gratefully acknowledges Yuanxin Xia and Vicente Cutanda Henriquez for their valuable assistance during instrumentation preparation.

References

[1] Barrera Figueroa, S., Rosell, A. T., Rasmussen, K., Jacobsen, F., and Cutanda Henriquez, V., "A practical implementation of microphone free-field comparison calibration according to the standard IEC 61094-8," in *INTER-NOISE 2012 Proceedings*, Acoustical Society of America, 2012.

[2] Saba, F., Durando, G., Prato, A., Schiavi, A., Corallo, M., and Paesante, D., "An experimental setup for the metrological characterization of MEMS microphones," in *2022 IEEE 9th International Workshop on Metrology for Industry 4.0 & IoT (MetroInd4.0 & IoT)*, pp. 156–160, Trento, Italy, 2022, doi:10.1109/MetroInd4.0IoT54463.2022.9831739.

[3] JCGM, "Evaluation of measurement data — Guide to the expression of uncertainty in measurement," 2008, doi:10.59161/JCGM100-2008E.

[4] BIPM, IEC, IFCC, ILAC, ISO, IUPAC, IUPAP, and OIML, "International Vocabulary of Metrology — Basic and general concepts and associated terms (VIM)," Joint Committee for Guides in Metrology, JCGM 200:2012. (3rd edition), 2012, doi: 10.59161/JCGM200-2012.

[5] Brüel & Kjær A/S, *Microphone Handbook: For the Falcon^{TM} Range of Microphone Products*, Nærum, Denmark, 1994, publication No. BE 1372–12.

[6] Sonion A/S, "P11AC03 Microphone Datasheet," Technical Datasheet Item-Configuration No. 3980-3203321, Version 3, Sonion A/S, Roskilde, Denmark, 2019, version date: 21 May 2019.

[7] Galetto, M., Schiavi, A., Genta, G., Prato, A., and Mazzoleni, F., "Uncertainty evaluation in calibration of low-cost digital MEMS accelerometers for advanced manufacturing applications," *CIRP Annals*, 68, pp. 535–538, 2019, ISSN 00078506, doi: 10.1016/j.cirp.2019.04.097.

[8] Schoukens, J., Rolain, Y., and Pintelon, R., "Analysis of windowing/leakage effects in frequency response function measurements," *Automatica*, 42, pp. 27–38, 2006, ISSN 00051098, doi:10.1016/j.automatica.2005.08.004.